J Electr Eng Technol Vol. 9, No. 6: 1900-1908, 2014
http://dx.doi.org/10.5370/JEET.2014.9.6.1900

ISSN(Print) 1975-0102
ISSN(Online) 2093-7423

A Water-Wall Model of Supercritical Once-Through Boilers Using Lumped Parameter Method

Geon Go* and Un-Chul Moon†

Abstract – This paper establishes a compact and practical model for a water-wall system comprising supercritical once-through boilers, which can be used for automatic control or simple analysis of the entire boiler-turbine system. Input and output variables of the water-wall system are defined, and balance equations are applied using a lumped parameter method. For practical purposes, the dynamic equations are developed with respect to pressure and temperature instead of density and internal energy. A comparison with results obtained using APESS, a practical thermal power plant simulator developed by Doosan Heavy Industries and Construction, is presented with respect to steady state and transient responses.

Keywords: Dynamic modelling, Supercritical once-through boiler, Water wall

1. Introduction

In spite of environmental issues, thermal power plants generate approximately 65% of the world's power supply. In recent years, the construction of large-capacity thermal power plants with environmental facilities has been common [1, 2].

With respect to structure, the boilers of thermal power plants are classified into two types: the drum boiler and the once-through boiler (OTB) [3]. Fig. 1 shows a schematic of a supercritical once-through boiler-turbine system. A supercritical once-through boiler comprises several heat exchangers, such as economizers, a water wall, superheaters, and reheaters. As shown in Fig. 1, the feedwater enters into the water wall through economizers. Then, the water is transformed into steam in the water-wall tube. The steam is superheated to generate electric power and circulated to the economizer again. Alternatively, a drum-type boiler system includes a drum, wherein saturated steam is separated from saturated fluid and provided to a superheater. The remaining saturated water re-enters the water-wall tubes through downcomers [4].

Currently, once-through boilers are constructed more commonly than drum boilers. Compared with drum boilers, once-through boilers can operate at higher pressure and temperature and thus allow greater energy efficiency. Because once-through boilers do not have drums or large-diameter downcomers, they exhibit less metal weight and smaller fluid storage capacity than drum boilers [5]. Therefore, although once-through boilers can respond rapidly to load changes, controlling them is more difficult than controlling drum boilers [6].

† Corresponding Author: School of Electrical and Electronic Engineering, Chung-Ang University, Korea. (ucmoon@cau.ac.kr)
* School of Electrical and Electronic Engineering, Chung-Ang University, Korea. (ggrock@cau.ac.kr)
Received: March 22, 2014; Accepted: September 15, 2014

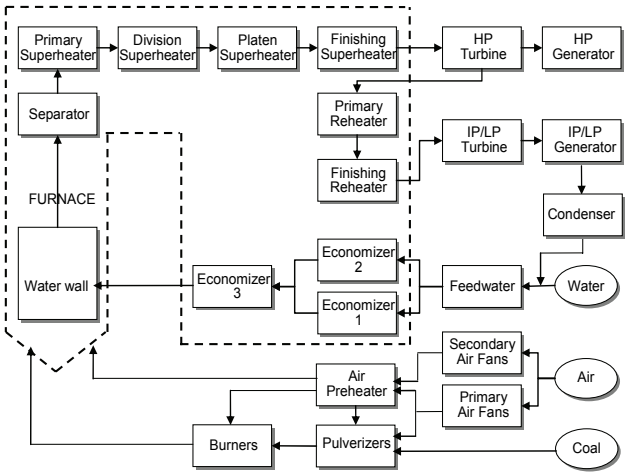

Fig. 1. Schematic of a supercritical once-through boiler-turbine system

In the system represented by Fig. 1, the entire surface of the lower part of the furnace wall is surrounded by water-wall tubes. When the operation conditions of the boiler exceed the critical point (22.09 MPa, 374.14°C [7]), the unit is called a "supercritical unit." In the water-wall tube of a supercritical once-through boiler, the phase of the water changes directly from liquid to vapor without undergoing saturation. This is a significant difference between the supercritical once-through boiler and other subcritical boilers. The water-wall system is one of the most important components affecting the dynamics of supercritical once-through boilers.

Although there are well-established models for drum boilers, such as those proposed by Bell and Åström [8], standard models for once-through boilers are far less common. Because of the major difference in the water-wall system between the two types of boilers, a compact and effective model of the water-wall system is currently a

relevant research topic.

There are many mathematical models of a water wall for subcritical once-through boilers [5, 9-11]; however, there are comparatively few mathematical models of a water wall for super-critical once-through boilers.

Dumont and Heyen developed an abridged mathematical model for the entire once-through boiler system [12]. They modified internal heat transfer coefficients and pressure drop formulations and considered the changes in the flow pattern. Li and Ren describe a water-wall system using a moving boundary [13]. They used enthalpy to track the moving boundary location at supercritical pressure and used mass, energy, and momentum balances to obtain the length of each section. Pan and colleagues presented a detailed water-wall model for predicting the mass flux distribution and metal temperature in the water wall of an ultra-supercritical boiler [14]. They treated the water-wall system as a network comprising 178 circuits, 15 pressure grids, and 7 connecting tubes; the system can be described using 195 non-linear equations.

Recently, intelligent systems have been applied for modelling a once-through boiler. Chaibakhsh and colleagues developed a model for a subcritical once-through boiler whose parameters are adjusted on the basis of genetic algorithms [15]. Lee and colleagues established a model for a large-scale power plant based on the neural network method [16], and Liu and colleagues described a supercritical once-through boiler using the fuzzy-neural network method [17].

In the present study, we attempt to develop a compact and practical model of water-wall systems for supercritical boilers that can be used for automatic control, analysis, and modeling of entire boiler-turbine systems. The objective is to develop a relatively simple water-wall model with sufficient accuracy for analysis and control rather than to describe the detailed dynamics occurring inside the water-wall tube. We use pressure and temperature as state variables; both of these are practical variables in industrial applications.

First, we establish input and output variables of water-wall systems and apply fundamental laws of physics, i.e., mass, energy, and momentum balance equations, using a lumped parameter method. Then, complicated equations and variables are approximated by adopting reasonable and applicable assumptions. To change the state variables with pressure and temperature, enthalpy and density are approximated as functions of pressure and temperature using a steam table. To verify the proposed model, a model of the water-wall system obtained using APESS, a practical thermal power plant simulator [18] developed by Doosan Heavy Industries and Construction, is presented and compared.

Table 1. Nomenclature

Roman and Greek Letters			
F [kg·s^2/kg·m^5]	Friction	T [ºC]	Temperature
H [kJ/kg]	Enthalpy	U [kJ/kg]	Internal Energy
L [m]	Length	V [m^3]	Volume
P [MPa]	Pressure	W [kg/s]	Mass Flow
Q [kJ/s]	Heat Flow	ρ [kg/m^3]	Density
Subscript			
aho	air preheater outlet	i	inlet
ave	arithmetic mean	o	outlet
eco	economizer outlet	ps(o)	primary superheater (outlet)
f	fluid	w	wall
fl	fuel	wf	wall to fluid
fn(o)	furnace (outlet)	ww(o)	water wall (outlet)
g	gas	wwgw	gas to wall at water wall
gw	gas to wall	wwwf	wall to fluid at water wall
Constants			
A_i [m^2]	Wall Inner Area		
A_o [m^2]	Wall Outer Area		
C_{vg} [kJ/kg ºC]	Specific Heat at Constant Volume of Flue Gas		
C_{vw} [kJ/kg ºC]	Specific Heat at Constant Volume of Wall		
K_{fl} [kJ/kg]	Calorific Value of Coal		
R_g [J/mol·K]	Gas Constant		
g [m/s^2]	Gravitational Acceleration		
g_c [kg·m/kgf·s^2]	Gravitational Conversion Factor		
h_f [W/ ºC·m^2]	Internal Heat Transfer Coefficient		
h_g [W/ ºC·m^2]	External Heat Transfer Coefficient		
ε [—]	Emittance of Flue Gas in Furnace		
σ [W/m^2 K^4]	Stefan-Boltzmann Constant		

2. Basic Balance Eqs. [3, 7, 19-22]

The fundamental principles used in developing the model are mass balance, energy balance, and momentum balance. Table 1 shows the nomenclature used in this paper. In Table 1, "wall" denotes the tube wall of each heat exchanger, such as the water wall, superheater, and reheater.

2.1 Mass balance

Mass balance is represented in (1), which gives the rate of mass change for a heat exchanger system.

$$W_i - W_o = V \frac{d\rho}{dt} \tag{1}$$

2.2 Energy balance

Energy balance is represented in (2), (4), and (6) for the combustion gas, tube wall, and working fluid, respectively. The dynamics of combustion gas are represented in (2), where Q_{gw} is the transferred heat flow from combustion gas to the tube wall. As shown in (3), Q_{gw} has two terms: radiative heat transfer and convective heat transfer. The temperature change of the tube wall is represented in (4), where Q_{wf} is the transferred heat flow from the tube wall to the internal working fluid in (5). Therefore, the combustion energy is represented as the temperature change of the tube

wall using (2) and (4). Finally, the dynamics of internal working fluid energy are represented in (6).

$$W_{gi}H_{gi} - W_{go}H_{go} - Q_{gw} = V_g C_{vg} \frac{d}{dt}(\rho_g T_g) \tag{2}$$

where,

$$Q_{gw} = \varepsilon\sigma A\left(T_g^4 - T_w^4\right) + h_g A\left(T_g - T_w\right) \tag{3}$$

$$Q_{gw} - Q_{wf} = V_w C_{vw} \rho_w \frac{d}{dt}(T_w) \tag{4}$$

where,

$$Q_{wf} = h_f A(T_w - T_f) \tag{5}$$

$$W_i H_i - W_o H_o + Q_{wf} = V \frac{d}{dt}(U\rho) \tag{6}$$

2.3 Momentum balance

The exact momentum balance of fluid in the tube is difficult to describe theoretically because of the internal turbulent flow of fluid. However, in the momentum balance equation, the dynamic term can be neglected because the pressure-flow process works faster than the mass and energy balance dynamics. In addition, the inertia term can be neglected compared with the friction term. These modifications result in the following equation, which is used in [19].

$$P_i - P_o = F\frac{W^2}{\rho} + \frac{L\rho g}{g_c} \tag{7}$$

Generally, heat exchangers in boiler systems, including a water wall, superheater, reheater, and economizer, can be modelled using (1) - (7). However, the major variables in these balance equations, such as pressure (P), temperature (T), density (ρ), enthalpy (H), and internal energy (U), are dependent variables that are functions of thermodynamic state. The thermodynamic state of water is classified into three state regions: the compressed liquid region, saturated liquid-vapor region, and superheated region. The saturated liquid-vapor region is called the "saturation region."

3. Development of a Water-Wall Model

3.1 Balance equations for water-wall systems

The detailed water-wall model considers many variables [12, 14]; in this paper, several major thermodynamic variables are selected on the basis of a lumped parameter method. To describe the simple water-wall system, several assumptions are required.

3.1.1 Assumptions

1. The pressure dynamics of the flue gas are negligible.
2. The flue gas exhibits ideal gas behavior.
3. The working fluid properties are uniform at any cross section.
4. The heat conduction in the axial direction is negligible.
5. The change in the thermodynamic properties of the internal working fluid is lumped.
6. The heat transfer from the flue gas to the wall is proportional to the combustion heat generated in the furnace.
7. The gas-wall heat transfer dynamics are sufficiently faster than the wall-fluid heat transfer dynamics.

The fundamental balance equations are modified according to the above assumptions. Four major variables — mass flow, enthalpy, pressure, and temperature at the outlet — are selected for both inputs and outputs. To consider the combustion energy, the mass flow of fuel (W_{fl}) is included as an input variable. The selected variables are represented in Fig. 2 and Table 2.

Therefore, in this paper, the water wall is represented as a 5-input and 4-output system. The fundamental balance Eqs. (1)-(7), are modified as follows.

3.1.2 Mass balance

Because the working fluid enters from the economizer, the inlet of the water wall is the outlet of the economizer. Therefore, the mass balance of the working fluid in the water wall, given by (1), is modified as follows:

$$V_{ww} \frac{d}{dt}(\rho_{wwo}) = W_{eco} - W_{wwo} \tag{8}$$

3.1.3 Energy balance

Regarding the energy balance of internal working fluid,

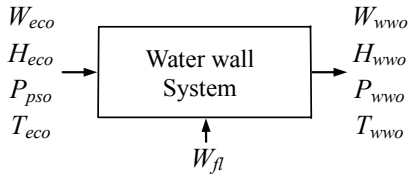

Fig. 2. Inputs and outputs of the water-wall model

Table 2. Inputs and outputs of water-wall system

Inputs ($\bar{U}$)	$W_{eco}(u_1)$	mass flow of economizer outlet
	$H_{eco}(u_2)$	enthalpy of economizer outlet
	$P_{pso}(u_3)$	pressure of primary superheater outlet
	$T_{eco}(u_4)$	temperature of economizer outlet
	$W_{fl}(u_5)$	mass flow of fuel
Outputs ($\bar{Y}$)	$W_{wwo}(y_1)$	mass flow of water wall outlet
	$H_{wwo}(y_2)$	enthalpy of water wall outlet
	$P_{wwo}(y_3)$	pressure of water wall outlet
	$T_{wwo}(y_4)$	temperature of water wall outlet

(6) can be written as follows:

$$V_{ww}\frac{d}{dt}(\rho_{wwo}U_{wwo}) = W_{eco}H_{eco} - W_{wwo}H_{wwo} + Q_{wwwf}, \quad (9)$$

where Q_{wwwf} is the transferred heat flow from the tube wall to the fluid, which is modified from (5) as

$$Q_{wwwf} = A_i h_f (T_w - T_f). \quad (10)$$

Regarding the dynamics of T_w, the temperature of the tube wall, given by (4), is rewritten as follows:

$$Q_{wwgw} - Q_{wwwf} = V_w C_{vw}\rho_w \frac{d}{dt}(T_w), \quad (11)$$

where Q_{wwgw} is the transferred heat flow from the flue gas to the tube wall. Then, Q_{wwgw} is

$$Q_{wwgw} = A_o \varepsilon\sigma\left(T_g^4 - T_w^4\right). \quad (12)$$

Regarding the dynamics of T_g in (12), (2) is modified as

$$W_g\left(H_{aho} - H_{fno}\right) - Q_{wwgw} + Q_c = V_{fn}C_{vg}\frac{d}{dt}(\rho_g T_g), \quad (13)$$

where Q_c is included to consider the heat input by the fuel combustion. In (13), because the flue gas comes from an air preheater and leaves the furnace, H_{aho} is the enthalpy at the air preheater outlet and H_{fno} is the enthalpy at the furnace outlet. Because there is no mass flow change of the flue gas in the furnace, W_{gi} and W_{go} in (2) are unified with W_g. Q_c is given as follows:

$$Q_c = K_{fl}W_{fl}, \quad (14)$$

where K_{fl} is the calorific value of fuel and W_{fl} is the fuel mass flow.

The energy balance Eqs. (8) - (14), can be directly used for the water-wall model. However, they require system variables from the other heat exchangers, such as the economizer, furnace, and air preheater, as well as additional system parameters such as heat transfer coefficients, the volumes of the furnace and wall, and the specific heat at constant volume of the wall and gas. Consequently, direct application of (8)-(12) results in a complicated model, which is beyond the scope of this paper.

In this study, to make the model more compact, we assume that the heat transfer from the gas to the tube wall is proportional to the combustion heat (assumption 6). Then, (12) can be expressed as follows:

$$Q_{wwgw} = \alpha Q_c, \quad (15)$$

where α is the ratio of Q_{wwgw} to Q_c. Although α can be considered a constant, it is a function of another thermal state [20]. In this study, α is a function of T_{ave}, which is the average temperature between two outlets. That is,

$$\alpha = \alpha(T_{ave}) = a_2 T_{ave}^2 + a_1 T_{ave} + a_0, \quad (16)$$

where,

$$T_{ave} = \frac{(T_{eco} + T_{wwo})}{2}. \quad (17)$$

The three coefficients a_i can be determined using the measurement data.

Typically, heat exchange between the gas and the wall is far faster than that between the wall and the fluid (assumption 7). Therefore, the dynamics of T_w can be ignored in (11) [3, 20]. Then, (11) is modified as a static equation with

$$Q_{wwwf} = Q_{wwgw}. \quad (18)$$

Accordingly, (18) can be expressed using (14) and (15) as follows:

$$Q_{wwwf} = \alpha(T_{ave})K_{fl}W_{fl} \quad (19)$$

$$= \eta(T_{ave})W_{fl}, \quad (20)$$

where, η represents the ratio of Q_{wwwf} to W_{fl}, which is equal to the product of α and K_{fl}.

As a result, the energy balance of the working fluid, given by (9), is simply represented using (20) as follows:

$$V_{ww}\frac{d}{dt}(\rho_{wwo}U_{wwo}) = W_{eco}H_{eco} - W_{wwo}H_{wwo} + \eta(T_{ave})W_{fl} \quad (21)$$

3.1.4 Momentum Balance

In the mass and energy balance equations, given in (8) and (21), the output variable W_{wwo} is determined using the momentum balance equation (7). Because the outlet of the water wall is the inlet of the primary superheater, the momentum balance of the working fluid at the primary superheater is given as follows:

$$P_{wwo} - P_{pso} = F_{ps}\frac{W_{wwo}^2}{\rho_{wwo}} + \frac{\rho_{wwo}L_{ps}g}{10.1972\cdot 10^4 \cdot g_c} \quad (22)$$

In (22), g and g_c represent gravitational acceleration and the gravitational conversion factor, respectively, whose values are approximately 9.80665 [m/sec^2] and 9.80665 [kg(mass)·m/kg(weight)·sec^2], respectively. The constant $10.1772\cdot 10^4$ is included in the denominator to change the units from [kg(weight)/m^2] to [MPa].

Although the friction factor, F_{ps}, in (22) is considered a constant [9, 19], F_{ps} is proportional to W_{eco} in practice. In

this study, F_{ps} is selected as a function of W_{eco}, as follows, to obtain better accuracy of the system:

$$F_{ps} = F_{ps}(W_{eco}) = b_1 W_{eco} + b_0 . \quad (23)$$

The two coefficients b_i can determined using the measurement data. Finally, three balance equations for the water-wall model are given by (8), (21), and (22) using (16), (20), and (23).

3.2 Change of state variables with *P* and *T*

The established model given by (8) and (21) explains the dynamics of density ρ and internal energy U of the working fluid. The state variables and the input and output variables are given as follows:

$$\bar{X} = [x_1, x_2] = [\rho_{wwo}, U_{wwo}] \quad (24)$$

$$\bar{U} = [u_1, u_2, u_3, u_4, u_5] = [W_{eco}, H_{eco}, P_{eco}, T_{pso}, W_{fl}] \quad (25)$$

$$\bar{Y} = [y_1, y_2, y_3, y_4] = [W_{wwo}, H_{wwo}, P_{wwo}, T_{wwo}] \quad (26)$$

In industrial practice, the pressure P and temperature T of the working fluid are directly measured and importantly managed. That is, the steam table is necessary to calculate ρ and U from measured variables. Because P and T are measured outputs, they can be directly compared with measured data for a real plant. Therefore, in this study, we set pressure and temperature as state variables of the water-wall system as follows:

$$\bar{X} = [x_1, x_2] = [P_{wwo}, T_{wwo}] \quad (27)$$

To change the state, ρ_{wwo} and U_{wwo} in dynamic equations (8) and (21) are set as functions of P_{wwo} and T_{wwo} in this study. Hereafter, the subscripts of ρ, U, P, T, and H are omitted for conciseness.

From the definition of enthalpy [7],

$$U = H - \frac{P}{\rho}, \quad (28)$$

the left side of (21) can be arranged as follows:

$$V_{ww}\frac{d}{dt}(\rho U) = V_{ww}\left[\rho\frac{d}{dt}(H - \frac{P}{\rho}) + (H - \frac{P}{\rho})\frac{d\rho}{dt}\right] \quad (29)$$

$$= V_{ww}\left[\rho\frac{dH}{dt} - \rho\frac{d}{dt}\frac{P}{\rho} + H\frac{d\rho}{dt} - \frac{P}{\rho}\frac{d\rho}{dt}\right] \quad (30)$$

$$= V_{ww}\left[\rho\frac{dH}{dt} + \frac{P}{\rho}\frac{d\rho}{dt} - \frac{dP}{dt} + H\frac{d\rho}{dt} - \frac{P}{\rho}\frac{d\rho}{dt}\right] \quad (31)$$

$$= V_{ww}\left[\rho\frac{dH}{dt} - \frac{dP}{dt} + H\frac{d\rho}{dt}\right] \quad (32)$$

Accordingly, (8) and (21) can be written as follows:

$$\frac{d\rho}{dt} = \frac{W_{eco} - W_{wwo}}{V_{ww}} \quad (33)$$

$$\rho\frac{dH}{dt} - \frac{dP}{dt} + H\frac{d\rho}{dt} = \frac{W_{eco}H_{eco} - W_{wwo}H_{wwo} + \eta(T_{ave})W_{fl}}{V_{ww}} \quad (34)$$

Then, a steam table is used to represent ρ and H in (33) and (34) as functions of P and T. Because the objective system operates in the superheated region, ρ and H of the superheated vapor region of the steam table are approximated as the following simple polynomial functions of P and T:

$$H = H(P,T) = c_3P + c_2T + c_1PT + c_o \quad (35)$$

$$\rho = \rho(P,T) = d_3P + d_2T + d_1PT + d_o , \quad (36)$$

where the coefficients are determined using the least squares method. These equations are valid only for the operation range used in the least squares method.

Using the chain rule,

$$\frac{dH}{dt} = \frac{\partial H}{\partial P}\frac{dP}{dt} + \frac{\partial H}{\partial T}\frac{dT}{dt}, \quad (37)$$

$$\frac{d\rho}{dt} = \frac{\partial \rho}{\partial P}\frac{dP}{dt} + \frac{\partial \rho}{\partial T}\frac{dT}{dt}, \quad (38)$$

and (33) and (34) are written as follows:

$$\frac{\partial \rho}{\partial P}\frac{dP}{dt} + \frac{\partial \rho}{\partial T}\frac{dT}{dt} = \frac{W_{eco} - W_{wwo}}{V_{ww}}, \quad (39)$$

$$\rho(\frac{\partial H}{\partial P}\frac{dP}{dt} + \frac{\partial H}{\partial T}\frac{dT}{dt}) - \frac{dP}{dt} + H(\frac{\partial \rho}{\partial P}\frac{dP}{dt} + \frac{\partial \rho}{\partial T}\frac{dT}{dt})$$

$$= \left[\rho\frac{\partial H}{\partial P} + H\frac{\partial \rho}{\partial P} - 1\right]\frac{dP}{dt} + \left[\rho\frac{\partial H}{\partial T} + H\frac{\partial \rho}{\partial T}\right]\frac{dT}{dt} \quad (40)$$

$$= \frac{W_{eco}H_{eco} - W_{wwo}H_{wwo} + \eta(T_{ave})W_{fl}}{V_{ww}} . \quad (41)$$

Next, dp/dt and dT/dt are determined using (39) and (41) with simple algebraic calculations as follows:

$$\frac{dP}{dt} = \frac{A\left(\rho\frac{\partial H}{\partial T} + H\frac{\partial \rho}{\partial T}\right) - B\frac{\partial \rho}{\partial T}}{\frac{\partial \rho}{\partial P}\left(\rho\frac{\partial H}{\partial T} + H\frac{\partial \rho}{\partial T}\right) - \frac{\partial \rho}{\partial T}\left(\rho\frac{\partial H}{\partial P} + H\frac{\partial \rho}{\partial P} - 1\right)}, \quad (42)$$

$$\frac{dT}{dt} = \frac{B\frac{\partial \rho}{\partial P} - A\left(\rho\frac{\partial H}{\partial P} + H\frac{\partial \rho}{\partial P} - 1\right)}{\frac{\partial \rho}{\partial P}\left(\rho\frac{\partial H}{\partial T} + H\frac{\partial \rho}{\partial T}\right) - \frac{\partial \rho}{\partial T}\left(\rho\frac{\partial H}{\partial P} + H\frac{\partial \rho}{\partial P} - 1\right)}, \quad (43)$$

where,

$$A = \frac{W_{eco} - W_{wwo}}{V_{ww}}, \quad (44)$$

$$B = \frac{W_{eco}H_{eco} - W_{wwo}H_{wwo} + \eta(T_{ave})W_{fl}}{V_{ww}} . \quad (45)$$

Then, we can rearrange the final water-wall equations with notations for state, input, and output as follows:

$$\frac{dx_1}{dt}=\frac{\begin{bmatrix}A(u_1,y_1)\{\rho(x_1,x_2)(c_2+c_1x_1)+y_2(d_2+d_1x_1)\}\\ -B(u_1,u_2,u_4,u_5,y_1,y_2,x_2)(d_2+d_1x_1)\end{bmatrix}}{\begin{bmatrix}(d_3+d_1x_2)\{\rho(x_1,x_2)(c_2+c_1x_1)+y_2(d_2+d_1x_1)\}\\ -(d_2+d_1x_1)\{\rho(x_1,x_2)(c_3+c_1x_2)+y_2(d_3+d_1x_2)-1\}\end{bmatrix}} \quad (46)$$

$$\frac{dx_2}{dt}=\frac{\begin{bmatrix}B(u_1,u_2,u_4,u_5,y_1,y_2,x_2)(d_3+d_1x_2)\\ -A(u_1,y_1)\{\rho(x_1,x_2)(c_3+c_1x_2)+y_2(d_3+d_1x_2)-1\}\end{bmatrix}}{\begin{bmatrix}(d_3+d_1x_2)\{\rho(x_1,x_2)(c_2+c_1x_1)+y_2(d_2+d_1x_1)\}\\ -(d_2+d_1x_1)\{\rho(x_1,x_2)(c_3+c_1x_2)+y_2(d_3+d_1x_2)-1\}\end{bmatrix}} \quad (47)$$

$$y_1=\sqrt{\frac{\rho(x_1,x_2)}{(b_1u_1+b_0)}\left(x_1-u_3-\frac{\rho(x_1,x_2)L_{ps}g}{10.1972\cdot10^4\cdot g_c}\right)} \quad (48)$$

$$y_2=c_3x_1+c_2x_2+c_1x_1x_2+c_0 \quad (49)$$

$$y_3=x_1 \quad (50)$$

$$y_4=x_2 \quad (51)$$

where,

$$A(u_1,y_1)=\frac{u_1-y_1}{V_{ww}} \quad (52)$$

$$B(u_1,u_2,u_4,u_5,y_1,y_2,x_2)=\frac{u_1u_2-y_1y_2+\eta(u_4,x_2)u_5}{V_{ww}} \quad (53)$$

$$\eta(u_4,x_2)=\left\{\frac{a_2(u_4+x_2)^2}{4}+\frac{a_1(u_4+x_2)}{2}+a_0\right\}K_{fl} \quad (54)$$

$$\rho(x_1,x_2)=d_3x_1+d_2x_2+d_1x_1x_2+d_0 \quad (55)$$

4. Simulation Results

To test the validity of the presented model, the water-wall system obtained using the APESS simulator is modeled as a target system. The presented water-wall model (46) - (55) is realized using MATLAB and a fourth-order Runge-Kutta algorithm is applied for the discrete simulation. Then, the steady-state and transient responses in superheated operation are compared.

For the simulation, three constants, V_{ww}, K_{fl}, and L_{ps}, are determined using the APESS simulator. The coefficients a_i for η and b_i for F_{ps} are determined using off-line data from APESS in the superheated operation range. The results of interpolation using the least squares method are as follows:

$$\eta=\eta(T_{ave})=1.058T_{ave}^2-8.1925\cdot10^2T_{ave}+1.6842\cdot10^5, \quad (56)$$

$$F_{ps}=F_{ps}(W_{eco})=8.1653\cdot10^{-7}W_{eco}-1.3784\cdot10^{-4}. \quad (57)$$

Fig. 3 shows the measurements and plot of η, and Fig. 4 shows the measurements and plot of F_{ps}. These two figures indicate that the interpolation is quite effective when considering real constants. In Fig. 4, the measurement value of F_{ps} changes from $2.8\cdot10^4$ to $4.5\cdot10^4$ according to the operating conditions, which explains why we do not use a constant F_{ps} in this study.

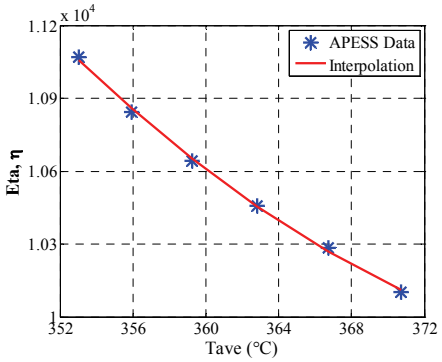

Fig. 3. η as a function of T_{ave}

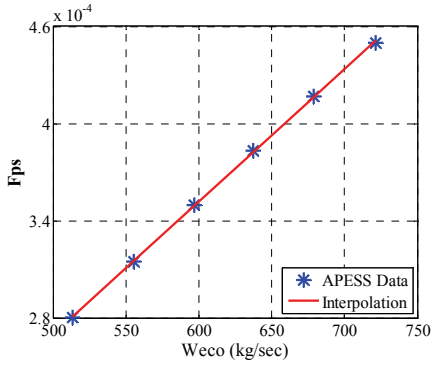

Fig. 4. F_{ps} as a function of W_{eco}

The coefficients c_i for H and d_i for ρ are also determined using the least squares method with the steam table. The regions $410°C<T_{wwo}<430°C$ and $25MPa<P_{wwo}<31MPa$ in the steam table are selected to simulate the operation range of APESS. The results of the approximation are as follows:

$$H=H(P,T)=-554.71P-23.27T+1.21PT+13697.48, \quad (58)$$

$$\rho=\rho(P,T)=246.70P+12.95T-0.5495PT-5709.504 \quad (59)$$

Eqs. (46)-(59) form the basis for the water-wall system in APESS. To verify the performance of the system, two types of simulations are tested: steady state responses and transient responses.

4.1 Steady-state test

For the steady-state comparison, the APESS model is run with fixed electric power generation. Because the APESS system has internal control loops, all variables in APESS are stabilized to a steady state. Then, steady-state values of the 5 inputs and 4 outputs of the water-wall system are obtained from APESS. The same input values are applied to the presented model, and steady-state output values are compared.

Table 3 shows a comparison between the APESS system and the presented model. In the table, electric power is

varied from 1000 MW to 800 MW, with which the boiler operates in the supercritical region. In Table 3, W_{wwo}, P_{wwo}, and T_{wwo} are directly proportional to the electric power, whereas H_{wwo} is inversely proportional. Percent errors of outputs are also presented, calculated as follows: |Model-APESS|/APESS. In the table, W_{wwo} and P_{wwo} exhibit relatively small errors compared with H_{wwo} and T_{wwo}. The maximum error is 0.27% (1.14 °C) for T_{wwo} with power generation of 900 MW. The average of all steady state errors is calculated to be 0.05%. Although there is no absolute criteria to determine modeling mismatch, we believe that these results are sufficient for predicting the steady state of the water-wall system.

Table 3. Steady-state values of APESS and model

Steady State Electric Power		W_{wwo} (kg/sec)	H_{wwo} (kJ/kg)	P_{wwo} (MPa)	T_{wwo} (°C)
1000 MW	APESS	722.0165	2628.043	30.4431	427.7541
	Model	722.0185	2630.294	30.4803	427.7730
	Error (%)	0.000277	0.085653	0.122195	0.004418
950 MW	APESS	679.0522	2641.539	29.1398	423.6766
	Model	679.0535	2638.269	29.1377	424.3435
	Error (%)	0.000191	0.12379	0.00721	0.157408
900 MW	APESS	638.9427	2657.184	27.8439	419.6174
	Model	638.9438	2654.154	27.8315	420.7609
	Error (%)	0.000172	0.11403	0.04453	0.27251
850 MW	APESS	596.9131	2678.955	26.6282	416.3527
	Model	596.9143	2677.901	26.6158	417.2913
	Error (%)	0.000201	0.03934	0.04657	0.225434
800 MW	APESS	556.5872	2705.929	25.3714	413.3563
	Model	556.5883	2708.836	25.3731	413.2225
	Error (%)	0.0002	0.10732	0.0067	0.03238

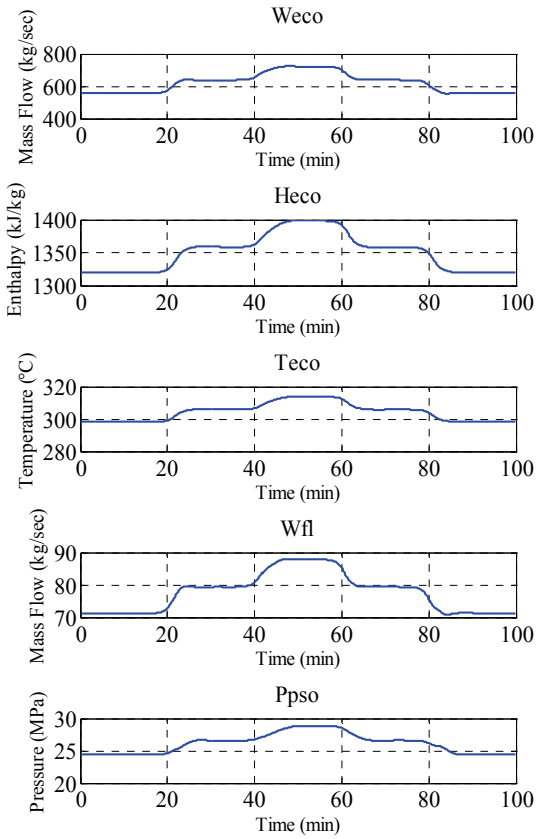

Fig. 5. Five input signals for transient responses.

4.2 Transient response test

For the comparison of transient responses, the electric load demand of APESS is increased and decreased in steps. The load demand signal is adjusted as follows: 800 MW → 900 MW → 1000 MW → 900 MW → 800 MW. Each step is maintained for 20 minutes to attain a new steady state. Fig. 5 shows graphs of the 5 inputs of the water-wall system obtained using APESS. The 5 inputs shown in Fig. 5 are applied to the presented model.

Figs. 6-9 show a comparison between the APESS model and the presented model. According to these figures, the responses of the four outputs are similar to those of a first-order system. Considering that (46) and (47) are very complicated, we find that the major dynamics of the water-wall system are quite simple.

According to Figs. 6 and 8, the responses of W_{wwo} and P_{wwo} are almost identical, as suggested by the steady-state responses. In Fig. 7, the initial value of enthalpy is not identical to the APESS data because the enthalpy is calculated using the pressure and temperature obtained by the approximated equation (58). Although the responses H_{wwo} and T_{wwo} exhibit different steady states, they have similar patterns with similar rising times.

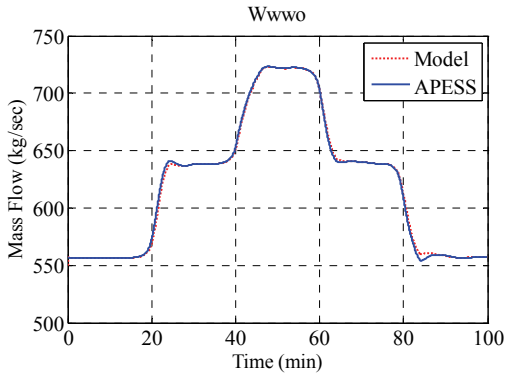

Fig. 6. Mass flow (W_{wwo}) of APESS and model

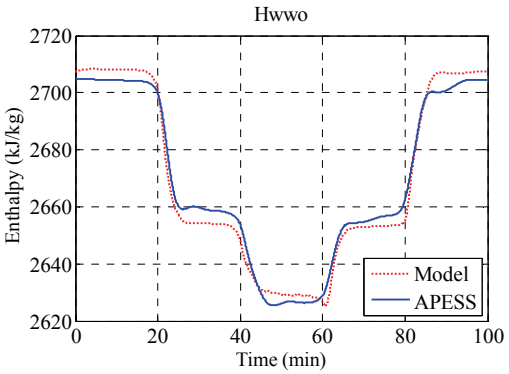

Fig. 7. Enthalpy (H_{wwo}) graphs of APESS and model

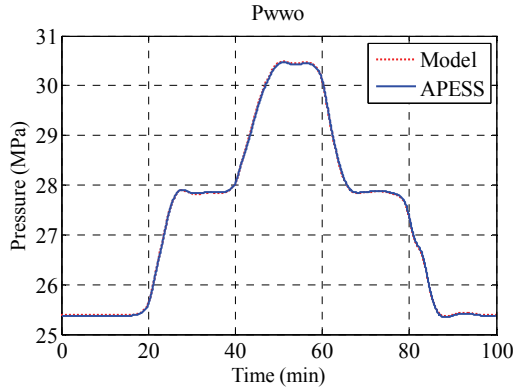

Fig. 8. Pressure (P_{wwo}) graphs of APESS and model.

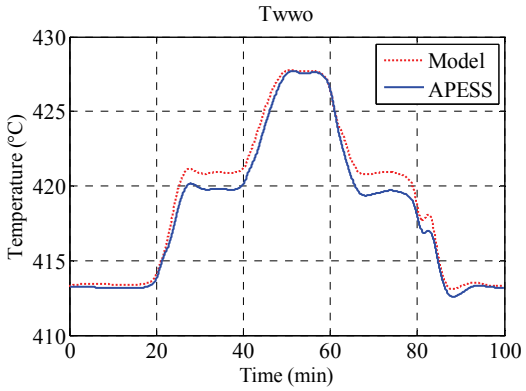

Fig. 9. Temperature (T_{wwo}) graphs of APESS and model.

5. Conclusion

We present a lumped model for the water-wall systems of supercritical once-through boilers. The model has two states, 5 inputs, and 4 outputs determined using a lumped parameter method. A steam table is approximated and used in the model equations to change the state.

A water-wall system obtained using the APESS simulator is modeled as a target system. Comparison results consider both steady states and transient responses. In both simulations, the mass flow and pressure exhibited similar results, and enthalpy and temperature exhibited small errors.

Although the presented model is quite complex, its dynamics are similar to those of a first-order system. We believe that this model is useful for designing an automatic controller and for analysis of water-wall systems.

Acknowledgements

This research was supported by the Chung-Ang University Excellent Student Scholarship and by the Chung-Ang University Research Grant in 2013, and by Basic Science Research Program through the National Research Foundation of Korea (NRF) funded by the Ministry of Education, Science and Technology (Grant Number: NRF-2010-0025555) .

References

[1] Changliang Liu and Hong Wang, "An Overview of Modeling and Simulation of Thermal Power Plant", *Proc.of IEEE International Conference on Advanced Mechatronic Systems*, pp. 86-91, Zhengzhou, China, 2011.

[2] H. Bentarzi, R.A. and Chentir and A. Ouadi, "A New Approach Applied to Steam Turbine Controller in Thermal Power Plant", *2nd International Conference on Control, Instrumentation and Automation*, pp. 86-91, Shiraz, Iran, 2011.

[3] J. Robert, W. Tobias, and O. Veronica, "Dynamic Modelling of Heat Transfer Processes in a Supercritical Steam Power Plant", M.S. thesis, Dept. Energy and Environment, Chalmers University of Technology, Göteborg, Sweden, 2012.

[4] R.A. Naghizadeh, B. Vahidi, and M.R.B. Tavakoli, "Estimating the Parameters of Dynamic Model of Drum Type Boilers Using Heat Balance Data as an Educational Procedure", *IEEE Trans. on Power Systems*, Vol. 26, No.2, pp. 775-782, May 2011.

[5] J. Adams, D.R. Clark, J.R. Louis, and J.P. Spanbauer, "Mathematical Model of Once-Through Boiler Dynamics", *IEEE Trans. on Power Systems*, Vol. 84, No. 2, pp. 146-156, 1965.

[6] Xu Cheng, R.W. Kephart, and C.H. Menten, "Model-based Once-through Boiler Start-up Water Wall Steam Temperature Control", *Proc. of IEEE International Conference on Control Applications*, pp. 778-783, Anchorage, Alaska, U.S.A., Sep. 2000.

[7] R.E. Sonntag, G.J. Van Wylen and C. Borgnakke, *Fundamentals of Thermodynamics*, John Wiley & Sons, Inc., 2002.

[8] R. D. Bell and K. J. Åström, *Dynamic models for boiler-turbine-alternator units: Data logs and parameter estimation for a 160 MW unit*, Report: TFRT-3192, Lund Institute of Technology, Sweden. 1987.

[9] A. Ray and H.F. Bowman, "A Nonlinear Dynamic Model of a Once-Through Subcritical Steam Generator", *ASME Trans. on Dynamic Systems, Measurement, and Control*, Vol. 98, pp. 332-339, Sep. 1976.

[10] J.M. Jensen and H. Tummescheit, "Moving Boundary Models for Dynamic Simulations of Two-Phase Flows", *Proc. Of the 2nd Int. Modelica Conference*, pp. 235-244, Oberpfaffenhofen, Germany, March 2002.

[11] S. Zheng, Z. Luo, X. Zhang and H. Zhou, "Distributed parameters modeling for evaporation system in a once-through coal-fired twin-furnace boiler", *International Journal of Thermal Sciences*, Vol. 50, pp. 2496-2505, 2011.

[12] M.N. Dumont and G. Heyen, "Mathematical modelling and design of an advanced once-through heat

recovery steam generator", *Computers & Chemical Engineering*, Vol. 28, pp. 651-660, 2004.
[13] Yong-Qi Li and Ting-Jin Ren, "Moving Boundary Modeling Study on Supercritical Boiler Evaporator: By Using Enthalpy to Track Moving Boundary Location", *Power and Energy Engineering Conference*, pp. 1-4, Wuhan, China, 2009.
[14] J. Pan, D. Yang, H. Yu, Q.C. Bi, H.Y. Hua, F. Gao and Z.M. Yang, "Mathematical modeling and thermal-hydraulic analysis of vertical water wall in an ultra supercritical boiler", *Applied Thermal Engineering*, Vol. 27, pp. 2500-2507, 2009.
[15] A. Chaibakhsh, A. Ghaffari and A.A. Moosavian, "A simulated model for a once-through boiler by parameter adjustment based on genetic algorithms", *Simulation Modelling Practice and Theory*, Vol. 15, pp. 1029-1051, 2007.
[16] K.Y. Lee, J.S. Heo, J.A. Hoffman, S.H. Kim and W.H. Jung, "Neural Network-Based Modeling for A Large-Scale Power Plant", *Power Engineering Society General Meeting*, IEEE, pp.1-8, 2007.
[17] X.J. Liu, X.B. Kong, G.L. Hou and J.H. Wang, "Modeling of a 1000MW power plant ultra supercritical boiler system using fuzzy-neural network method", *Energy Conversion and Management*, Vol. 65, pp. 518-527, 2013.
[18] K.Y. Lee, J.H. Van Sickel, J.A. Hoffman, W.H. Jung and S.H. Kim, "Controller Design for a Large-Scale Ultrasupercritical Once-Through Boiler Power Plant", *IEEE Trans. on Energy Conversion*, Vol. 25, No. 4, pp. 1063-1070, Dec., 2010.
[19] Patrick Benedict Usoro, "Modeling and Sumulation of a Drum Boiler-Turbine Power Plant under Emergency State Control", M.S. thesis, Dept. Mechanical Engineering, Massachusetts Institute of Technology, Cambridge , United States of America, 1977.
[20] W. Shinohara and D.E. Koditschek, "A Simplified Model of a Supercritical Power Plant", University of Michigan, Control group reports, CGR-95-08, 1995.
[21] H. Li, X. Huang and L. Zhang, "A lumped parameter dynamic model of the helical coiled once-through steam generator with movable boundaries", *Nuclear Engineering and Design*, Vol. 238, pp. 1657-1663, 2008.
[22] J.H. Hwang, "Drum Boiler Reduced Model: a Singular Perturbation Method", *20th International Conference on Electronics, Control and Instrumentation*, Vol. 3, pp. 1960-1964, Bologna, Italy, Sep. 1994.

Geon Go received his B.S. degree in Electrical and Electronics Engineering from Chung-Ang University, Seoul, Korea, in 2013. He is currently an M.S Candidate in Electrical and Electronics Engineering at Chung-Ang University. His research interests involve the operation and modeling of fossil power plants and power system analysis.

Un-Chul Moon received his B.S., M.S., and Ph.D. degrees from Seoul National University, Korea, in 1991, 1993, and 1996, respectively, all in Electrical Engineering. In 2000, he joined Woo-Seok University, Korea, and in 2002, he joined Chung-Ang University, Korea, where he is currently an Associate Professor of Electrical Engineering. His current research interests are power system analysis, computational intelligence, and automation.